Journal of Fluorescence (2020) 30:1075–1083
https://doi.org/10.1007/s10895-020-02578-z

ORIGINAL ARTICLE

Multifunctional ZnO/SiO_2 Core/Shell Nanoparticles for Bioimaging and Drug Delivery Application

A. P. S. Prasanna[1] · K. S. Venkataprasanna[1] · Balashanmugam Pannerselvam[2] · Vijayshankar Asokan[3] · R. Sofia Jeniffer[4] · G. Devanand Venkatasubbu[1]

Received: 29 April 2020 / Accepted: 23 June 2020 / Published online: 3 July 2020
© Springer Science+Business Media, LLC, part of Springer Nature 2020

Abstract

Semiconducting nanoparticles with luminescent properties are used as detection probes and drug carriers in in-vitro and in-vivo analysis. ZnO nanoparticles, due to its biocompatibility and low cost, have shown potential application in bioimaging and drug delivery. Thus, ZnO/SiO_2 core/shell nanoparticle was synthesised by wet chemical method for fluorescent probing and drug delivery application. The synthesised core/shell nanomaterial was characterized using XRD, FTIR, UV-VIS spectroscopy, Raman spectroscopy, TEM and PL analysis. The silicon shell enhances the photoluminescence and aqueous stability of the pure ZnO nanoparticles. The porous surface of the shell acts as a carrier for sustained release of curcumin. The synthesized core/shell particle shows high cell viability, hemocompatibility and promising florescent property.

Keywords Bioimaging · Core/shell · Sustainable drug release · Biocompatible

Introduction

Bioimaging technique has been widely used to investigate the cellular, physio-chemical functions and morphology with the help of organic dyes and fluorescence proteins [1]. But these organic dyes and protein are highly susceptible to photobleaching, short stokes shift, decomposition and poor photochemical stability due to frequent excitation which makes them unsuitable for long-term cell imaging applications [2, 3]. So, researches have developed different techniques such as magnetic resonance imaging, fluorescence imaging, computed tomography radio imaging, etc., that enables better visualization of cells [4]. The use of luminescent nanomaterial in fluorescence imaging outstands the other techniques due to its high sensitivity, real-time imaging, and minimal-invasiveness. Among them, semiconductor quantum dots such as CdSe and CdTe have been widely used due to its high extinct coefficient, quantum yield, photo-stability, narrow emission, tuneable emission wavelength, and single-source excitation [5, 6]. But the use of cadmium (Cd) based quantum dots in biological application was limited due to its adverse toxic effect like generation of reactive oxygen species, water-insolubility and release of Cd^{2+} ions [7–9]. Hence to overcome these limitations alternative fluorescence techniques and material needs to be developed.

Among the group II-VI semiconductors ZnO is an alternative material for Cd based fluorescent imaging. It has a with a wide bandgap of 3.37 eV and 60 meV of exciton binding energy [10]. Due to its unique property it provides various application in different fields such as electronics, optoelectronics, laser, sensors, energy generators, etc. [11, 12]. The biocompatibility and biodegradable property of ZnO have pave a path for its potential biological application in various domain like skincare, tissue regeneration, antimicrobial and anticancer activity, biosensors, fluorescence probes, and drug delivery [13–15]. ZnO shows weak excitonic photoemission in the UV region and a broad multiple defect-related to visible

A. P. S. Prasanna and K. S. Venkataprasanna contributed equally to this work.

✉ G. Devanand Venkatasubbu
gdevanandvenkatasubbu@gmail.com

[1] Department of Physics and Nanotechnology, SRM Institute of Science and Technology, Chengalpattu District, Tamil Nadu 603 203, India

[2] Centre for Nanoscience and Technology, Anna University, Chennai, Tamil Nadu, India

[3] Department of Chemistry and Chemical Engineering, Chalmers University, Gothenburg, Sweden

[4] Center of Nanotechnology Research (CNR), VIT University, Vellore, Tamilnadu, India

luminescence under ambient conditions. But the weak visible emission is due to the surface defect and water instability nature that reduces the potential use of ZnO in florescence imaging [7, 10]. ZnO emits weak green light under UV excitation due to its surface defect [16]. ZnO fluorescence is easily destroyed in wider pH that is present in our biological system and thus appropriate surface modifications are required to stabilize ZnO fluorescence [17]. Therefore, the most effective way to achieve water stable and photostable ZnO is by coating it with a wider bandgap material like silica (SiO_2) to form core/shell structure [18].

Core/shell nanostructure have gained attention from the past two decades as it can be operated as a multifunctional nanomaterial. Due to its distinguished property core/shell nanomaterials are used in various applications like sensors, electronics, optoelectronics, catalysis, biomedical, etc. [19, 20]. The size and width of the shell influence the surface charge, surface reactivity, stability, and dispersive ability of the core. The advantage of core/shell nanoparticle in the biomedical applications are (i) low cytotoxicity (ii) improved hydrophilicity for bio and cytocompatibility (iii) surface modification and functionalization and (iv) high chemical stability [21].

SiO_2 was selected as a shell due to its biocompatibility, water stability, surface chemistry, wider bandgap and ease to functionalization. Moreover, silica shells block the diffusion of molecules from the core and the shell which reduces the toxic effect of the nanoparticles [1, 22]. The growth of inorganic SiO_2 over ZnO nanoparticles improves the photoluminescence yield, photostability of the nanoparticles by reducing the nonradiative recombination. In addition to that, the surface to volume ratio of porous SiO_2 nanoparticle facilitates better surface functionalization through covalent bonding or electrostatic interaction. Silanol groups present on the surface of the SiO_2 make it hydrophilic which makes it water stable. Some of the anticancer drugs like curcumin, camptothecin, and paclitaxel are hydrophobic and these hydrophobic drugs can bind to the SiO_2 pores structure by hydrogen bonding and electrostatic interaction which makes it stable in water and in turn aids in drug delivery [23]. In this article, curcumin is used as a drug due to its nontoxic and biocompatible behaviour. It is also used as an anti-inflammatory drug, chemotherapeutics, antimicrobial agent, anti-oxidant, antiarthritic and thrombus suppressive agent [24, 25].

In this paper, we have prepared ZnO and ZnO/SiO_2 core/shell nanoparticles by wet chemical synthesis for bioimaging applications. The synthesized core/shell nanoparticles were characterized using spectroscopy, structural, surface, and microscopy techniques. Curcumin (an anticancer drug) is loaded on the SiO_2 shell as a drug for drug delivery application where the drug loading and realizing property were studies along with its florescence property. The cytocompatibility and hemocompatibility of the core/shell material was futured analyzed.

Experimental

Synthesis of ZnO Nanoparticle

ZnO nanoparticles were prepared by the co-precipitation method. A stock solution of 8% (*W*/*V*) Zinc Nitrate solution was prepared to which 2 M of Sodium hydroxide solution was added dropwise and stirred continuously for 2 h. A white precipitate was obtained and it was washed several times with ethanol and deionized water. Followed by drying the sample at 40 °C in hot air oven.

Synthesis of ZnO/SiO_2 Core/Shell Nanoparticle

1% (*W*/*V*) of the prepared ZnO nanoparticle was dispersed in water: ethanol solution of ratio 1:9. It was then ultrasonicated for 30 min. Then the solution was stirred. 5 ml of NH_4OH was added to the solution and stirred for 30 min. 0.25 g of CTAB was added to the solution. After 30 min of stirring, 0.2 ml of TEOS was added to the solution in a dropwise manner and stirred continuously for 24 h. Then the solution was washed several times with deionized water and dried at 80 °C in hot air oven [26].

Drug Loading

Curcumin loaded ZnO/SiO_2 core/shell nanoparticle were prepared by, dissolving 100 mg of curcumin in 100 ml of dichloromethane. After stirring 100 mg of ZnO/SiO_2 core/shell nanoparticle was added slowly and stirred for 24 h. After continuous stirring the resultant solution was centrifuged, washed and dried under vacuum to obtained Curcumin loaded ZnO/SiO_2 core/shell nanoparticle. The amount of curcumin loaded in ZnO/SiO_2 core/shell nanoparticle was obtained by measuring the absorbance at 420 nm (standard curve for curcumin is made separately). The drug loading percentage was calculated using the below formula.

Drug loading (%) = [(A-B)/A] * 100.

where A and B represent the initial and final drug concentration of the aqueous drug solution.

Drug Release Study

To determine the drug release profile, 50 mg of curcumin loaded ZnO/SiO_2 core/shell nanoparticles was taken in 100 ml phosphate-buffered saline (PBS) medium under sterile condition. The drug release was studied for 35 h. At every one hour interval 5 ml of the sample was taken and replaced immediately with the fresh buffer. The amount of drug released was measured spectroscopically. Curcumin concentration was measured at 420 nm [27].

Hemocompatibility Assay

10 ml of blood was obtained from a healthy volunteer. Hemolysis assay is carried out in a solution containing 5 ml of fresh ACD (acid citrate dextrose) human blood diluted with a 5 ml 0.9% saline solution which is kept as stock. The prepared sample (20 μg/ml) was mixed with 4 ml of saline solution and incubated at 37 °C for 30 min. The 0.3 ml of stock solution was added to the tubes containing the sample and incubated at 37^0 C. The measurement was done at different time intervals (60,120,180 min). 100% hemolysis and 0% hemolysis are represented as positive and negative control, respectively. It is prepared by diluting 0.3 ml of stock solution with 5 ml of Triton X 100 and 5 ml of saline solution, respectively. At 1500 rpm, the solutions obtained were centrifuged for 5 min, and the supernatant absorbance was measured at 545 nm. The oxyhaemoglobin content's absorbance is reported at 545 nm. The samples were performed and analysed in triplicate. The formula employed to estimate hemolysis was:

$$\text{Hemolysis}\ (\%) = \left[\frac{OD_{test} - OD_{neg}}{OD_{pos} - OD_{neg}}\right] \times 100$$

Where,

OD_{neg} denotes absorption of 0% lysis.

OD_{pos} denotes absorption of 100% lysis.

OD_{test} denotes the absorption of the synthesised samples [34].

Cytotoxicity Analysis

The NIH 3 t3 fibroblast cells were seeded in 96-well microplates with a cell density of 1×10^4 cells/well and incubated for 24 h at 37 °C in 5% CO_2 incubator. After attaining 80% of confluency, the medium was replaced with ZnO/SiO_2 core/shell nanoparticles of different concentrations (5, 10, 15, 20, and 25 μg/mL) and incubated for 24 h. The cells were then washed with phosphate buffer saline solution. 20 μL of (MTT) solution (5 mg/mL) was added to each well and incubated for 4 h. The formazan crystal was solubilized by adding 100 μL DMSO and the absorbance was measured at 570 nm. The percentage of cell viability was calculated using the below formula [28].

$$Cell\quad viability(\%) = \frac{Absorbance\quad of\quad treated\quad cells}{Absorbance\quad of\quad control\quad cells} x100$$

Cellular Imagine

The NIH 3 t3 fibroblast cells were seeded in culture dishes (60 mm) with a cell density of 1×10^6 cells/well and incubated at 37 °C in an incubator containing 5% CO_2. After 70–85% of cell growth, the cells were harvested by trypsinization followed by washing it with PBS solution. The obtained cells were then seeded (1×10^4 cells) in cover slip and incubated at 37 °C in the 5% CO_2 incubator, followed by washing and fixing the cells with 3.6% formaldehyde for 15 min. Then the coverslips were added with ZnO/SiO_2 core/shell nanomaterial (5 μg/mL) and imaged under microscope.

Results and Discussion

Figure 1 shows the XRD image of pure ZnO and ZnO/SiO_2 nanoparticles. The crystalline peaks of ZnO at 32.14°, 34.59°, 36.78°, 48.02°, 57.08°, 63.43°, 68.57°, 69.78°, 73.44°, and 77.61° corresponds to the crystal planes (100), (002), (101), (102), (110), (103), (200), (112), (201), (202) and (104) respectively. The peaks obtained at (100), (002) and (101) indicates that the synthesised ZnO is of Wurzite structure. Characteristic peaks of other crystalline phases of ZnO or any other impurity peaks were not observed. The sharp and strong intense crystalline peaks indicate the strong crystalline nature of ZnO nanocrystal. The XRD pattern of ZnO/SiO_2 shows no characteristic peak of SiO_2 but comparatively the intensities of the pure ZnO peaks reduces. This indicates the reduction in crystalline nature of ZnO. The hump between 20 to 30 indicates the presence of SiO_2 (amorphous) and it matches with the previous results. TEM analysis further confirms that presence of SiO_2 [20, 29, 30].

Figure 2 (a) represents the FTIR spectrum of pure ZnO and ZnO/SiO_2 nanostructure. ZnO shows single characteristic vibration mode between 430 to 520 cm^{-1}. The peak at 477 cm^{-1} belongs to the symmetric stretching of Zn-O. Due to the absorption of methane, ZnO forms H3CH-Zn^{2+} ions which gives rise to the C-H vibrational mode at 1387 cm^{-1} and bending of C- H at 837 cm^{-1} [31]. In ZnO/SiO_2 nanostructure, the vibration of the Si-O-Si bridge can be witnessed around 1000–1230 cm^{-1}. This indicates the presence of SiO_2 in ZnO/

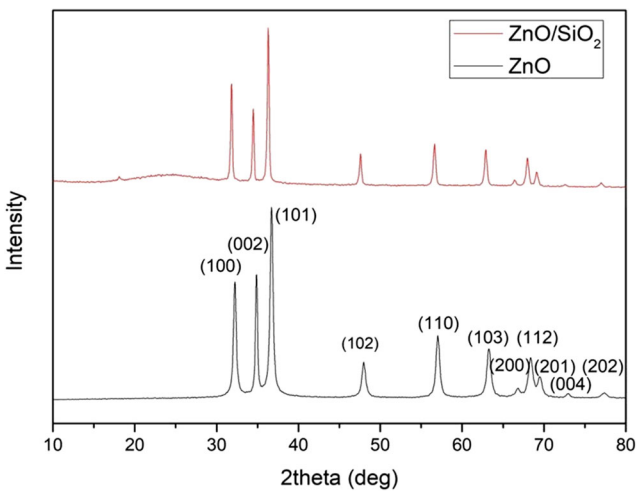

Fig. 1 **a** XRD image of ZnO and ZnO/SiO_2

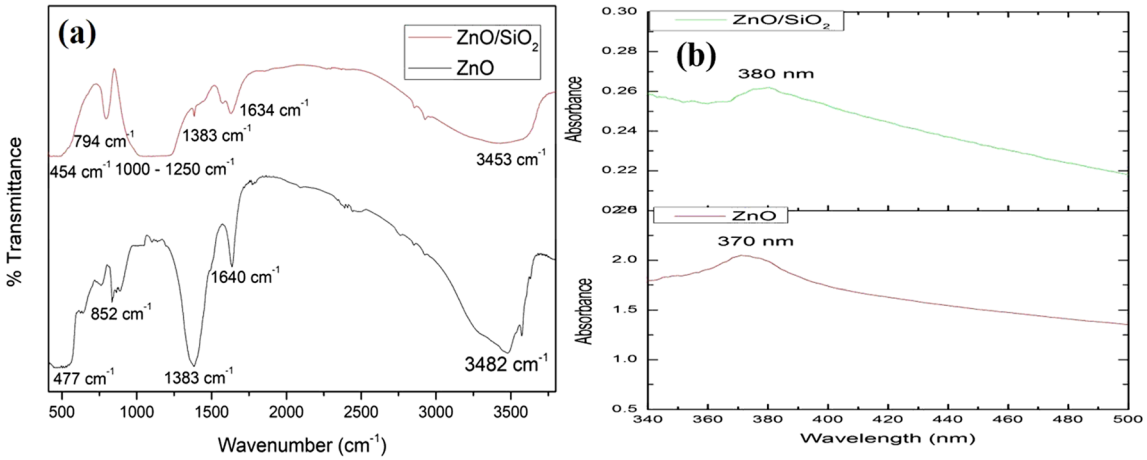

Fig. 2 **a** FTIR image of ZnO and ZnO/SiO_2, **b** UV spectrum of ZnO nanoparticle and ZnO/SiO_2 nanostructure

SiO_2. The bands at 1632 cm^{-1} and 3466 cm^{-1} belongs to –OH bending and stretching respectively [20, 29, 30].

Figure 2 (b) represents the UV spectrum of pure ZnO nanoparticle and ZnO/SiO_2 nanostructure. UV absorption of ZnO

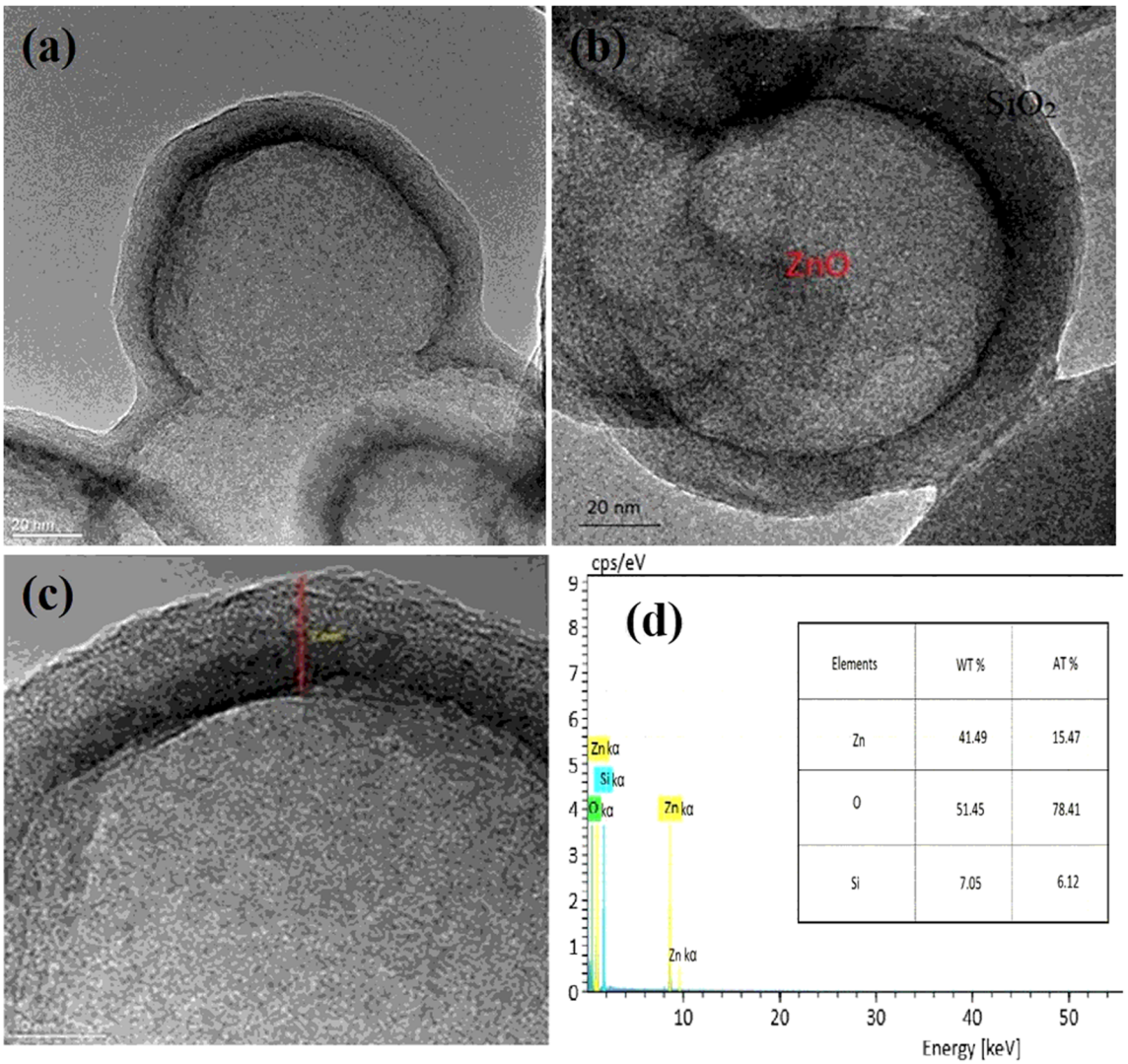

Fig. 3 **a**, **b** and **c** TEM image of ZnO/SiO_2 Nanoparticles and **d** EDS elemental mapping of ZnO/SiO_2 core/shell nanoparticle.

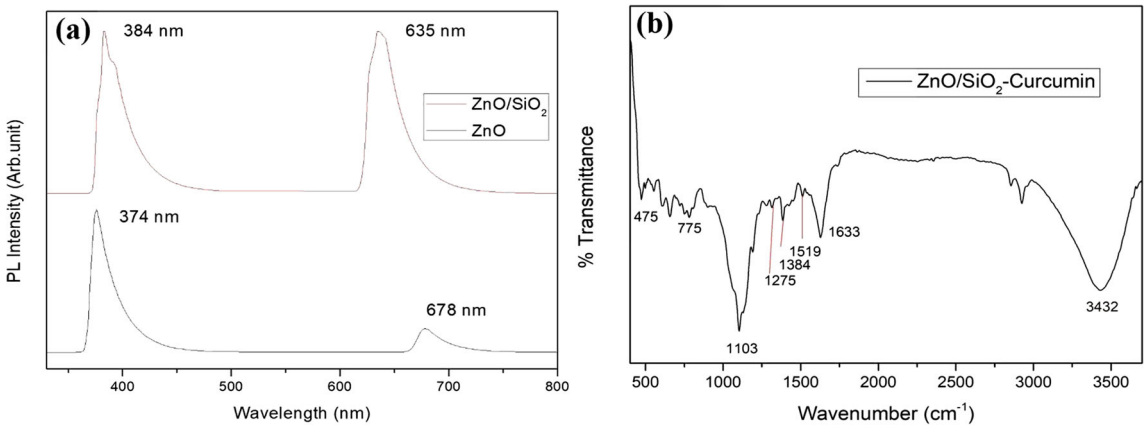

Fig. 4 **a** PL spectra of ZnO and ZnO/SiO_2 core/shell nanoparticle and **b** FTIR Spectra Curcumin loaded ZnO/SiO_2 core/shell nanoparticle

varies from 350 nm to 400 nm due to various factors like size, structure and synthesis techniques. In this study pure ZnO absorption occurs at 370 nm. A shift of 10 nm in the absorbance can be observed in ZnO/SiO_2 core/shell nanoparticles when compared to the pure ZnO. This redshift is due to the change in the excitation energy of the ZnO. The change in the excitation energy could be due to the ultrasonication process which was used to synthesised ZnO/SiO_2 nanostructure [31–33].

Figure 3 (a, b, and c) represents the TEM image of ZnO/SiO_2 core/shell nanoparticles. The TEM image conforms the synthesised sample is of core/shell nanostructure. ZnO core has a diameter of 60 nm and the width of the shell was 7–10 nm. The elemental analysis (EDX) study was performed for ZnO/SiO_2 core/shell nanoparticle and was shown in Fig. 3 (d). The result confirms the presence of Zn, O, and Si elements.

Photoluminescence analysis of pure ZnO and ZnO/SiO_2 core/shell nanoparticles at room temperature with an excitation wavelength of 325 nm is given in Fig. 4 (a). PL spectra of ZnO exhibits two emission peaks. The first emission is between 370 and 420 nm. This corresponds to the bandgap excitonic emission. The second emission is between 450 and 680 nm (red emission) which is due to the defect states of ZnO among which Zn interstitial and oxygen vacancies defects are the predominant ionic defects. In ZnO/SiO_2 core/shell nanoparticles excitation-emission was observed around 384 nm. The red emission at 637 nm matches with the pure ZnO nanoparticles. This red emission occurring in both ZnO and ZnO/SiO_2 core/shell nanoparticles. This is due to the Zn_i to O_i transition [34, 35].

Figure 4 (b) shows the FTIR Spectra of Curcumin loaded ZnO/SiO_2 core/shell nanoparticle. The predominant peak of ZnO was observed at 475 cm^{-1}. The signature peak of curcumin was observed around 1505 cm^{-1}. This attributes to the C=O and C=C vibrations. The enol peaks are at 1275 cm^{-1} (C-O vibration). Due to the interaction between SiO_2 and curcumin, the broad peak of Si-O-Si bridge vibration between 1000 and 1230 cm^{-1} is narrowed (at 1103 cm^{-1}). The peaks at 1633 cm^{-1} and 3432 cm^{-1} belongs to the bending and stretching mode of –OH group respectively [24, 34, 36].

Nitrogen adsorption-desorption isotherm and pore size distribution performed for ZnO/SiO_2 core/shell nanoparticle and curcumin loaded ZnO/SiO_2 core/shell nanoparticle are shown

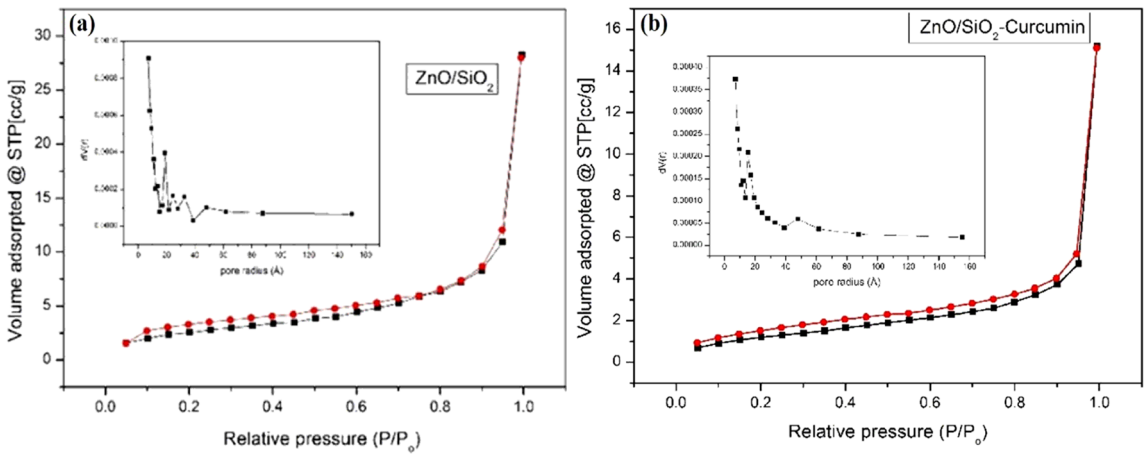

Fig. 5 **a** Nitrogen adsorption-desorption isotherm and pore size distribution of ZnO/SiO_2 core/shell nanoparticle and **b** Nitrogen adsorption-desorption isotherm and pore size distribution of Curcumin loaded ZnO/SiO_2 core/shell nanoparticle

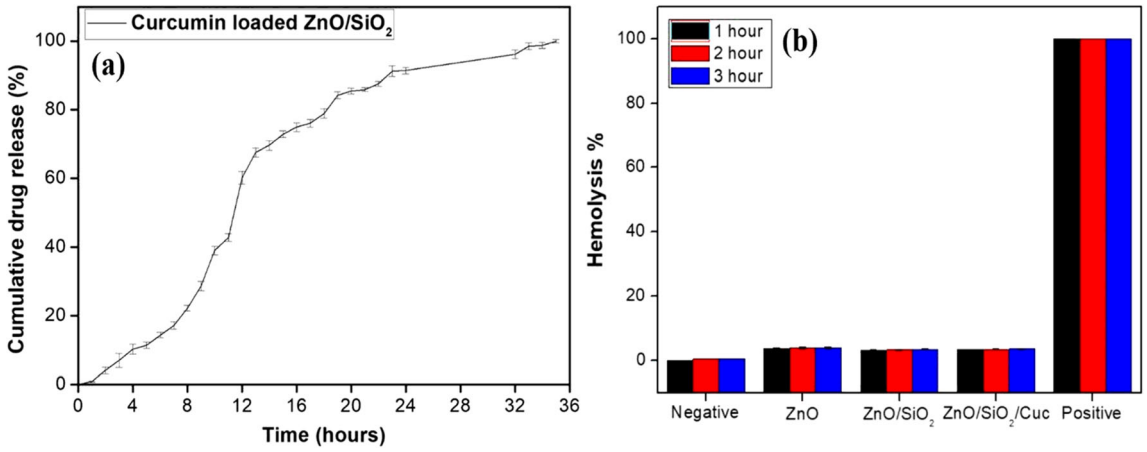

Fig. 6 **a** Drug release profile of curcumin and **b** Hemolysis percentage of ZnO, ZnO/SiO_2 and Curcumin loaded ZnO/SiO_2

in Fig 5 (a & b). Pore size distribution curve of ZnO/SiO_2 core/shell nanoparticle were sized under 50 Å, which confirms that the ZnO/SiO_2 core/shell nanoparticle is mesoporous. The total pore volume of ZnO/SiO_2 core/shell nanoparticle for pores with a radius of less than 53.28 Å is 9.796 cc g^{-1}. Curcumin loaded ZnO/SiO_2 core/shell nanoparticle have a total pore volume of 4.503e-03 cc g^{-1}. The pores radius is less than 53.00 Å The change in the pore volume confirms that curcumin is loaded in the pores of SiO_2 of ZnO/SiO_2 core/shell nanoparticle.

The amount of curcumin present in 100 mg of ZnO/SiO_2 core/shell nanostructure was calculated and found to be 65 mg. The FTIR analysis conforms the presence of the drug in the core/shell nanostructure. In addition to that, the Nitrogen adsorption-desorption isotherm and pore size distribution confirm the presence of the curcumin in the porous surface of the SiO_2 which in-turn reduces the pore size distribution in the shell. The absorption of curcumin in the shell might be due to hydrogen bonding, electrostatic interaction, and the weak vander-wall force between the shell and the drug.

Figure 6 (a) shows the drug release profile of curcumin loaded ZnO/SiO_2 core/shell nanoparticles. The high surface area and low toxicity of the SiO_2 makes it an appropriate material for drug delivery application. The drug release analysis of curcumin loaded ZnO/ SiO_2 was carried out in the PBS solution. The drug gets attached to the surface of the silica shell due to hydrogen bonding and electrostatic interaction. When it is exposed to the system (PBS at pH 7.4) the desorption of drug takes place. The interaction between the drug (curcumin) and the pores in the SiO_2 surface decrease as the drug gets attached to the hydrophobic surface of the cells (biological system) which eventually detach the drug from the silica surface in a sustained manner. The drug release profile clearly explains the rate of drug release at each point of time. Initially, the drug release starts after 1 h as the drug needs time to attain sufficient surface energy to break the bond between the drug and the silicon shell. Within 12 h 50% of the

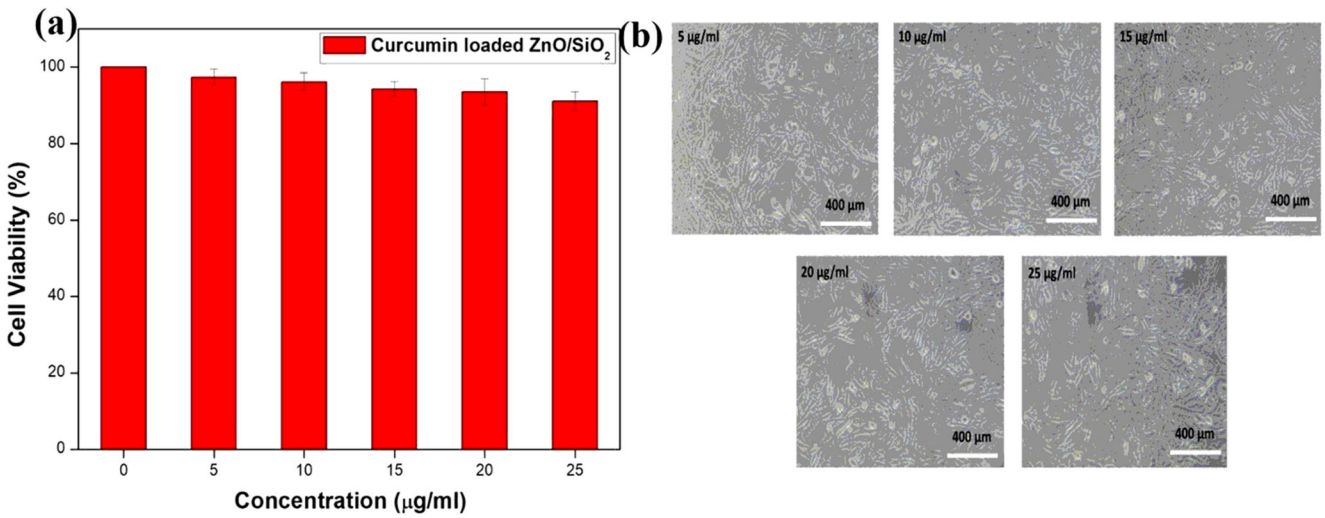

Fig. 7 **a** Cytotoxicity assay on NIH3t3 fibroblast cells treated with ZnO/SiO_2 nanoparticles, and **b** microscopy images of NIH3t3 fibroblast cells treated with ZnO/SiO_2 nanoparticles at various concentration

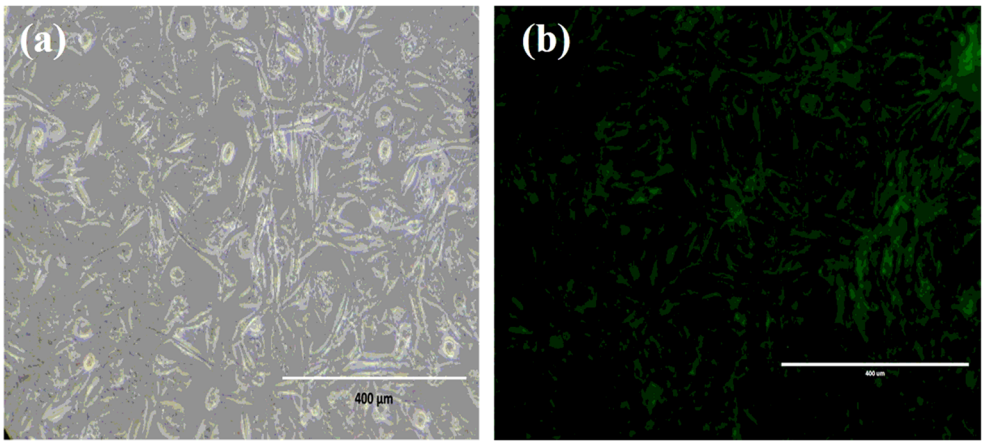

Fig. 8 **a** and **b** Florescence images of Curcumin loaded ZnO/ SiO_2 in NIH3t3 fibroblast cells with green emission.

drug is released and at 25th hour nearly 80% of the drug release is witnessed. After 25 h the elution of the drug from the ZnO/ SiO_2 gets slower due to the difference in the concentration gradient. But as the time increase, 98.8% of the drug release is achieved at the 35th hour. Thus, we can conclude that a sustained drug release of 80% of the drug occurs within 24 h. This analysis shows the variance of $P < 0.001$.

Figure 6 (b) shows the hemocompatibility analysis of the ZnO, ZnO/ SiO_2 and curcumin loaded ZnO/ SiO_2 nanomaterials. 20 µg/ml of samples were taken and treated with fresh human blood at different time interval (1,2 and 3 h). Less than 5% of erythrocyte lysis is permissible for biomaterials. ZnO ^{shows} nearly 3.7% RBC lysis in the first hour and then becomes steady (3.9%) at 2nd and 3rd hour. ZnO/ SiO_2 shows 3.5% of RBC lysis after 3 h of incubation. The erythrocyte lysis is less for ZnO/ SiO_2 when compare to pure ZnO. This is because of its biocompatible nature. The SiO_2 core prevents the leaching from the interior core. Curcumin loaded ZnO/ SiO_2 showed a result similar to that of ZnO/ SiO_2 with a slight variation of 0.18%. This shows that the prepared nanomaterials were hemocompatible.

Figure 7 (a) shows the cytotoxicity analysis of curcumin loaded ZnO/ SiO_2 against NIH3t3 fibroblast cells. The non-toxic nature of ZnO and SiO_2 were readily shown in the cytotoxicity assay. Material that shows nearly 80% of cell viability can be used in the biological system and can be classified as a biomaterial. Thus, different concentrations (5, 10, 15, 20, 25 µg/ml) of curcumin loaded ZnO/ SiO_2 nanoparticles were incubated with fibroblast cells for 24 h. For 5 µg/ml 97.5% of cell viability is observed. For 10, 15 and 20 µg/ml nearly 96%, 94.25% and 92% of cell were viable. 90% of cell viability was noted for 25 µg/ml. Figure 7 (b) show the normal optical image of the fibroblast cells treated with different concentrations of curcumin loaded ZnO/ SiO_2 nanoparticles. The changes in cell morphology were negligible. Thus, this study concludes that the prepared core/shell nanomaterial does not show any toxic effect on the fibroblast cells and can be used for bioimaging applications.

Figure 8 (a and b) shows the confocal fluorescence imaging of NIH3t3 fibroblast cell in presence of curcumin loaded ZnO/ SiO_2 nanoparticles. The cells were cultured and incubated with curcumin loaded ZnO/ SiO_2 nanoparticles at 5 µg/ml concentration. ZnO shows a bandgap excitonic emission and defect emission between 370 and 420 nm and 450–680 nm respectively. The coating of inorganic wide-bandgap silica shell enhances the emission spectrum which is noted by the redshift in the emission. Yellow, blue, and green emission of ZnO had been reported elsewhere depending upon the size, morphology and method of synthesis. The synthesized core/shell nanoparticle is incubated with the cells and was analyzed under the confocal microscope. Green emission is witnessed in the cells due to the recombination and transition between the photoexcited hole and single charged oxygen valency in the nanomaterials. The further reason for the green emission can be the combination of the peak at 380 (blue color) and 635 nm (yellowish-orange color). Thus, it clearly shows that even at minimum concentration curcumin loaded ZnO/ SiO_2 nanoparticles shows high fluorescence property and the nanomaterial gets well attached to the cells and produce broadly visible luminescence.

Conclusion

Multifunctional curcumin loaded ZnO/ SiO_2 core/shell nanoparticles were successfully synthesised and characterized. TEM analysis confirms the synthesised nanomaterial is of core/shell structure. The cytotoxicity and the hemocompatibility assay conclude the biocompatible nature of ZnO/SiO_2 core/shell nanoparticles. Curcumin loaded ZnO/ SiO_2 nanoparticles shows high visible florescence even at lower concentration. The sustained release of curcumin from ZnO/ SiO_2 core/shell nanoparticles makes it suitable for targeted drug delivery application.

Acknowledgements The authors APS Prasanna, K S Venkataprasanna and G. Devanand Venkatasubbu thanks department of physics and nanotechnology for providing lab facilities.

Compliance with Ethical Standards

Conflict of Interest There are no conflicts to declare.

References

1. Zhang ZY, Xiong HM (2015) Photoluminescent ZnO nanoparticles and their biological applications. Materials 8(6):3101–3127
2. Tang X, Choo ESG, Li L, Ding J, Xue J (2010) Synthesis of ZnO nanoparticles with tunable emission colors and their cell labeling applications. Chem Mater 22(11):3383–3388
3. Deshmukh K, Shaik MM, Ramanan SR, Kowshik M (2016) Self-activated fluorescent hydroxyapatite nanoparticles: a promising agent for bioimaging and biolabeling. ACS Biomater Sci Eng 2(8):1257–1264
4. Kherlopian AR, Song T, Duan Q, Neimark MA, Po MJ, Gohagan JK, Laine AF (2008) A review of imaging techniques for systems biology. BMC Syst Biol 2(1):74
5. Aldeek F, Mustin C, Balan L, Medjahdi G, Roques-Carmes T, Arnoux P, Schneider R (2011) Enhanced photostability from CdSe (S)/ZnO core/shell quantum dots and their use in biolabeling. Eur J Inorg Chem 6:794–801
6. Salman MS, Riaz A, Iqbal A, Zulfiqar S, Sarwar MI, Shabbir S (2017) Design and fabrication of covalently linked PEGylated nanohybrids of ZnO quantum dots with preserved and tunable fluorescence. Mater Des 131:156–166
7. Pan ZY, Liang J, Zheng ZZ, Wang HH, Xiong HM (2011) The application of ZnO luminescent nanoparticles in labeling mice. Contrast Media Mol Imaging 6(4):328–330
8. Bagalkot V, Zhang L, Levy-Nissenbaum E, Jon S, Kantoff PW, Langer R, Farokhzad OC (2007) Quantum dot− aptamer conjugates for synchronous cancer imaging, therapy, and sensing of drug delivery based on bi-fluorescence resonance energy transfer. Nano Lett 7(10):3065–3070
9. Fu A, Gu W, Boussert B, Koski K, Gerion D, Manna L, Le Gros M, Larabell CA, Alivisatos AP (2007) Semiconductor quantum rods as single molecule fluorescent biological labels. Nano Lett 7(1):179–182
10. Layek A, De S, Thorat R, Chowdhury A (2011) Spectrally resolved photoluminescence imaging of ZnO nanocrystals at single-particle levels. J. Phys Chem Lett 2(11):1241–1247
11. Özgür Ü, Alivov YI, Liu C, Teke A, Reshchikov M, Doğan S, Avrutin VCSJ, Cho SJ, Morkoç AH (2005) A comprehensive review of ZnO materials and devices. J Appl Phys 98(4):11
12. Siddiquey IA, Furusawa T, Sato M, Bahadur NM, Alam MM, Suzuki N (2012) Sonochemical synthesis, photocatalytic activity and optical properties of silica coated ZnO nanoparticles. Ultrason Sonochem 19(4):750–755
13. Jiang J, Pi J, Cai J (2018) The advancing of zinc oxide nanoparticles for biomedical applications. Bioinorg Chem Appl 2018:1–18
14. Padmanabhan A, Kaushik M, Niranjan R, Richards JS, Ebright B, Devanand Venkatasubbu G (2019) Zinc oxide nanoparticles induce oxidative and proteotoxic stress in ovarian cancer cells and trigger apoptosis independent of p53-mutation status. Appl Surf Sci 487:807–818
15. Kaushik M, Niranjan R, Thangam R, Madhan B, Pandiyarasan V, Ramachandran C, Oh DH, Devanand Venkatasubbu G (2019) Investigations on the antimicrobial activity and wound healing potential of ZnO nanoparticles. Appl Surf Sci 479:1169–1177
16. Al Dine, EJ (2017). Synthesis and characterization of smart nanoparticles (Doctoral dissertation, Université de Lorraine; Université libanaise)
17. Ma YY, Ding H, Xiong HM (2015) Folic acid functionalized ZnO quantum dots for targeted cancer cell imaging. Nanotechnology 26(30):305702
18. Mulvaney P, Liz-Marzan LM, Giersig M, Ung T (2000) Silica encapsulation of quantum dots and metal clusters. J Mater Chem 10(6):1259–1270
19. Ghosh Chaudhuri R, Paria S (2011) Core/shell nanoparticles: classes, properties, synthesis mechanisms, characterization, and applications. Chem Rev 112(4):2373–2433
20. Galedari NA, Rahmani M, Tasbihi M (2017) Preparation, characterization, and application of ZnO@ SiO 2 core–shell structured catalyst for photocatalytic degradation of phenol. Environ Sci Pollut Res 24(14):12655–12663
21. Chatterjee K, Sarkar S, Rao KJ, Paria S (2014) Core/shell nanoparticles in biomedical applications. Adv Colloid Interf Sci 209:8–39
22. Morks MF (2008) Fabrication and characterization of plasma-sprayed HA/SiO2 coatings for biomedical application. J Mech Behav Biomed Mater 1(1):105–111
23. Li Z, Barnes JC, Bosoy A, Stoddart JF, Zink JI (2012) Mesoporous silica nanoparticles in biomedical applications. Chem Soc Rev 41(7):2590–2605
24. Devanand Venkatasubbu G, Anusuya T (2017) Investigation on Curcumin nanocomposite for wound dressing. Int J Biol Macromol 98:366–378
25. Li F, Huang X, Jiang Y, Liu L, Li Z (2009) Synthesis and characterization of ZnO/SiO2 core/shell nanocomposites and hollow SiO2 nanostructures. Mater Res Bull 44(2):437–441
26. Zhai J, Tao X, Pu Y, Zeng XF, Chen JF (2010) Core/shell structured ZnO/SiO2 nanoparticles: preparation, characterization and photocatalytic property. Appl Surf Sci 257(2):393–397
27. Niranjan R, Kaushik M, Prakash J, Venkataprasanna KS, Arpana C, Devan BP, Venkatasubbu G (2019) Enhanced wound healing by PVA/chitosan/Curcumin patches: in vitro and in vivo study. Colloids Surf B: Biointerfaces 182:110339
28. Venkataprasanna KS, Prakash J, Vignesh S, Bharath G, Venkatesan M, Banat F, Sahabudeen S, Ramachandran S, Devanand Venkatasubbu G (2019). Fabrication of chitosan/PVA/GO/CuO patch for potential wound healing application. Int J Biol Macromol 143:744–762
29. Raevskaya AE, Panasiuk YV, Stroyuk OL, Kuchmiy SY, Dzhagan VM, Milekhin AG, Yeryukov NA, Sveshnikova LA, Rodyakina EE, Plyusnin VF, Zahn DRT (2014) Spectral and luminescent properties of ZnO–SiO 2 core–shell nanoparticles with size-selected ZnO cores. RSC Adv 4(108):63393–63401
30. Scarano D, Bertarione S, Spoto G, Zecchina A, Arean CO (2001) FTIR spectroscopy of hydrogen, carbon monoxide, and methane adsorbed and co-adsorbed on zinc oxide. Thin Solid Films 400(1–2):50–55
31. Reinosa JJ, Leret P, Álvarez-Docio CM, Del Campo A, Fernández JF (2016) Enhancement of UV absorption behavior in ZnO–TiO2 composites. Bol Soc Esp Ceram Vidrio 55(2):55–62
32. Pei L, Huang Y, Li C, Zhang Y, Rasco BA, Lai K (2014). Detection of triphenylmethane drugs in fish muscle by surface-enhanced Raman spectroscopy coupled with Au-Ag core-shell nanoparticles Journal of Nanomaterials p3
33. Yoshikawa M, Inoue K, Nakagawa T, Ishida H, Hasuike N, Harima H (2008) Characterization of ZnO nanoparticles by resonant Raman scattering and cathodoluminescence spectroscopies. Appl Phys Lett 92(11):113115

34. Lim J, Bokare AD, Choi W (2017) Visible light sensitization of TiO 2 nanoparticles by a dietary pigment, curcumin, for environmental photochemical transformations. RSC Adv 7(52):32488–32495
35. Jangir LK, Kumari Y, Kumar A, Kumar M, Awasthi K (2017) Investigation of luminescence and structural properties of ZnO nanoparticles, synthesized with different precursors. Materials Chemistry Frontiers 1(7):1413–1421
36. Pandit RS, Gaikwad SC, Agarkar GA, Gade AK, Rai M (2015) Curcumin nanoparticles: physico-chemical fabrication and its in vitro efficacy against human pathogens. 3. Biotech 5(6):991–997

Publisher's Note Springer Nature remains neutral with regard to jurisdictional claims in published maps and institutional affiliations.